

1  
2 **Detecting snow-related signals in radial growth of *Pinus***  
3 ***uncinata* mountain forests**  
4  
5  
6

7 Alba Sanmiguel-Vallelado<sup>1</sup>, J. Julio Camarero<sup>1</sup>, Antonio Gazol<sup>1</sup>, Enrique Morán-  
8 Tejada<sup>2</sup>, Gabriel Sangüesa-Barreda<sup>3,1</sup>, Esteban Alonso-González<sup>1</sup>, Emilia Gutiérrez<sup>4</sup>,  
9 Arben Q. Alla<sup>5</sup>, J. Diego Galván<sup>6</sup>, Juan Ignacio López-Moreno<sup>1</sup>.

10  
11  
12  
13 <sup>1</sup> Pyrenean Institute of Ecology, IPE-CSIC, Avda. Montañana 1005, 50059 Zaragoza, Spain

14 <sup>2</sup> Department of Geography, University of the Balearic Islands, Carr. de Valldemossa km 7.5, 07122  
15 Palma de Mallorca, Spain

16 <sup>3</sup> Área de Botánica, Departamento de Ciencias Agroforestales, EiFAB,iuFOR-Universidad de Valladolid,  
17 Campus Duques de Soria, 42004 Soria, Spain

18 <sup>4</sup> Dept. Biologia Evolutiva, Ecologia i Ciències Ambientals, Univ. Barcelona, Av. Diagonal 643, 08028  
19 Barcelona, Spain

20 <sup>5</sup> Fakulteti i Shkencave Pyjore, Universiteti Bujqësor i Tiranës, 1029 Tirana, Albania

21 <sup>6</sup> Ionplus AG. Lerzenstrasse 12, 8953 Dietikon, Switzerland

22  
23  
24  
25  
26  
27 Corresponding author:  
28 Alba Sanmiguel-Vallelado  
29 albasv@ipe.csic.es  
30

31 **Abstract**

32 Climate warming is responsible for observed reduction in snowpack depth and an earlier  
33 and faster melt-out in many mountains of the Northern Hemisphere. Such changes in  
34 mountain hydroclimate could negatively affect productivity and tree growth in high-  
35 elevation forests, but few studies have investigated how and where recent warming trends  
36 and changes in snow cover influence forest growth. A network comprising 36 high-  
37 elevation *Pinus uncinata* forests was sampled in the NE Iberian Peninsula, mainly across  
38 the Spanish Pyrenees, using dendrochronology to relate tree radial growth to a detailed  
39 air temperature and snow depth data. Radial growth was negatively influenced by a longer  
40 winter snow season and a higher late-spring snowpack depth. Notably, the effect of snow  
41 on tree growth was found regardless the widely reported positive effect of growing-season  
42 air temperatures on *P. uncinata* growth. No positive influence of moisture from spring  
43 snowmelt on annual growth of *P. uncinata* was detected in sampled forests. Tall trees  
44 showed a lower growth responsiveness to snow than small trees. Decreasing trends in  
45 winter and spring snow depths were detected at most Pyrenean forests, suggesting that  
46 the growth of high-elevation *P. uncinata* forests can benefit for a shallower and of  
47 shorter duration snowpack associated with warmer conditions. However, water-limited  
48 sites located on steep slopes or on rocky substrates, with poor soil-water holding capacity,  
49 could experience drought stress because of early depleted snow-related soil moisture.

50

51 **Keywords:** dendroecology, tree-ring width, snowpack, subalpine forests, Pyrenees.

52

## 53 **1. Introduction**

54 Mountain forests are particularly susceptible to climatic variation because low  
55 temperatures typically limit radial growth and productivity near the uppermost edge of  
56 tree distribution ranges (Körner, 2012). Recent warming trends have induced shifts in tree  
57 recruitment (Smithers et al., 2018; Sangüesa-Barreda et al., 2018) and have enhanced  
58 radial growth (Innes, 1991; Tardif et al., 2003; Camarero et al., 2015a; Zhuang et al.,  
59 2017), excepting few sites where warming has induced some drought stress (Camarero et  
60 al., 2015c, Galván et al. 2015). Most studies have focused on the direct effects of rising  
61 temperatures on tree growth (e.g. Del Barrio et al., 1990; Gutierrez et al., 1991; Tardif et  
62 al., 2003; Andreu et al., 2007; Galván et al., 2014; Camarero et al., 2017; Franke et al.,  
63 2017; D'Orangeville et al., 2018; Sanchez-Salguero et al., 2018; Wang et al., 2019).  
64 Research focused on the indirect effects of climate warming, such as the influence of  
65 snow dynamics on forest productivity, is still scarce (Vaganov et al., 1999; Kirilyanov et  
66 al., 2003, Helama et al., 2013, Watson and Luckman 2016; Carlson et al., 2017).

67       Snow accumulation requires a combination of precipitation and low temperatures  
68 to initiate snowfall and persistent below-zero temperatures to sustain the snowpack  
69 (Beniston et al., 2011; López-Moreno et al., 2011). Due to the high sensitivity of snow  
70 cover to seasonal temperatures (Morán-Tejeda et al., 2013a), a warmer climate can easily  
71 impact the process of snow accumulation/melting (Beniston, 2003). An increase in winter  
72 temperature leads to a precipitation shift from snow towards rain, and warmer spring  
73 conditions induce earlier and faster snowpack melting (Morán-Tejeda et al., 2014).  
74 Reduced snowpack depth and duration have been reported in the main mid-latitude  
75 mountain ranges (López-Moreno, 2005; Marty, 2008; McCabe and Wolock, 2009;  
76 Beniston, 2012; Morán-Tejeda et al., 2013a) including Mediterranean (drought-prone)  
77 areas such as the Pyrenees (Morán-Tejeda et al., 2017).

78 Snow dynamics may influence forest growth (e.g., Kirdyanov et al., 2003). Early  
79 snowfalls in the autumn may shorten the growing season and lead to a reduction in the  
80 assimilation of carbohydrates, and this can negatively affect growth in the following year  
81 (Carlson et al., 2017). A lack of snow cover during the winter can cause premature  
82 yellowing and shedding of needles of shrubby krummholz individuals during cold and  
83 dry winters and repeated freeze-thaw cycles (winter drought), reducing growth in the  
84 following spring (Helama et al., 2013; Camarero et al. 2015b). Larger snow accumulation  
85 and a longer snowmelt period may negatively affect tree radial growth by slowing the  
86 increase of soil temperature, delaying the growing period, and thus shortening the  
87 growing season (Vaganov et al., 1999; Kirdyanov et al., 2003; Watson and Luckman,  
88 2016). On the other hand, snowmelt effects on soil moisture have been reported to  
89 positively influence tree growth during the next growing season (St. George, 2014;  
90 Watson and Luckman, 2016). All these observations suggest that the radial growth of  
91 trees can be related to winter snowpack, melt-out date and spring snow depth.

92 In the main mountains of the NE Iberian Peninsula (Pyrenees, Pre-Pyrenees, Iberian  
93 System), increasing trends in mean temperatures and an increment in precipitation  
94 variability have been observed during the second half of the 20th century (López-Moreno  
95 et al., 2010; El Kenawy et al., 2011). Such consequent water stress increase may also  
96 limit tree growth in high-elevation forests (Tardif et al., 2003; Andreu et al., 2007).  
97 Nevertheless, high-elevation mountain pine (*Pinus uncinata*) forests and treelines are  
98 forecasted to show enhanced growth during the late 21<sup>st</sup> century due to a longer and  
99 warmer growing season (Sánchez-Salguero et al., 2012, Camarero et al., 2017). Climate  
100 warming has also affected mountain hydrology and influences the accumulation, duration  
101 and melt-out of snow, leading to a shallow snowpack or a longer snow-free season  
102 (Morán-Tejeda et al., 2013a, 2013b). Discerning how and where snow dynamics affects

103 forest growth may help us understand future responses of mountain forests to forecasted  
104 hydroclimatic change.

105 The main hypothesis of the present study is that snowpack depth and duration  
106 influence radial growth of high-elevation *P. uncinata* forests. It was expected that snow  
107 cover affects tree radial growth, in addition to the widely reported temperature effects on  
108 growth (Gutiérrez, 1991; Rolland and Schueller, 1994; Camarero et al., 1998). It was also  
109 expected that there would be greater impact of snowpack depth and duration on growth  
110 in high-elevation forests with a shorter growing season, since elevation indirectly controls  
111 the effects of climate on *P. uncinata* growth by modifying growing season air temperature  
112 (Tardif et al., 2003; Galván et al., 2014). These hypotheses were tested by analyzing the  
113 radial growth of a *P. uncinata* dendrochronological network in the main mountain ranges  
114 of NE Iberia in relation to snow cover conditions at site level. The specific objectives of  
115 the present study were: (1) to evaluate the associations between snow conditions and  
116 radial-growth variability of *P. uncinata* forests; (2) to explore the influence of  
117 biogeographical patterns and tree characteristics on tree growth responses to snow depth;  
118 and (3) to estimate and compare the temporal evolution of radial growth and snow trends  
119 for the 1980-2010 period.

120

## 121 **2. Materials and methods**

### 122 *2.1. Study species*

123 The mountain pine (*Pinus uncinata* Ram.) is a long-lasting and light-demanding conifer,  
124 which shows a wide ecological tolerance regarding topography (slope, aspect, elevation)  
125 and soil type (Cantegrel, 1983) and forms high-elevation forests. The natural habitat of  
126 *P. uncinata* includes central and southwest European mountains, while its southern  
127 geographical limit is reached in the Iberian System (Spain). It is dominant in the subalpine

128 belt of the central and eastern Pyrenees (1800-2500 m a.s.l.). Its growing season starts at  
129 the end of May and ends in October, with major growth rates occurring from the end of  
130 May to July (Camarero et al., 1998). Warm autumn and spring temperatures before and  
131 during tree-ring formation enhance *P. uncinata* radial growth, whereas summer  
132 precipitation during the growing season is the main positive climate driver of growth in  
133 certain xeric sites located in the Pre-Pyrenees and southern Iberian System (Gutiérrez,  
134 1991; Camarero et al., 1998; Tardif et al., 2003; Andreu et al., 2007; Galván et al., 2014).  
135 The timing of *P. uncinata* tree-ring formation is schematized in Figure 1.

136

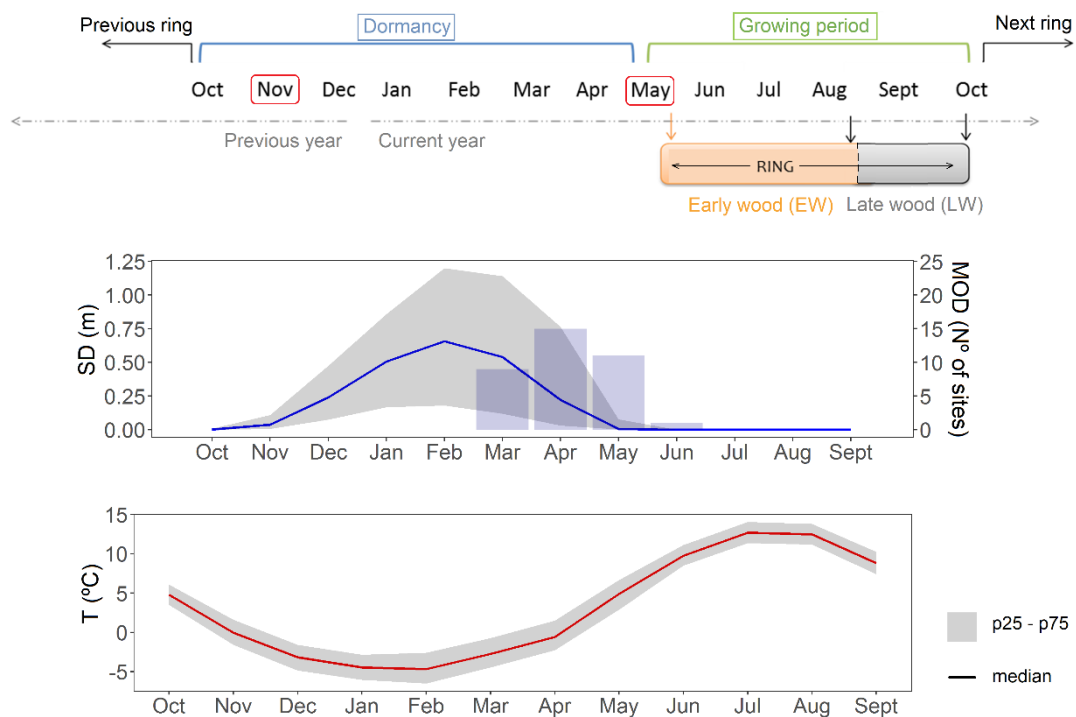
## 137 2.2. Study sites

138 The 36 studied forests are located in the main mountain ranges of the NE Iberian  
139 Peninsula (Figure 2): 33 are located in the Pyrenees, (3 of them in the Pre-Pyrenees, the  
140 Pyrenees' foothills), and the other 3 sites are located in the Iberian System. Two of the  
141 sites sampled in the southern Iberian system (VATE, VA1U) constitute the southernmost  
142 distribution limit of the species in Europe. Sampled sites cover the whole geographical  
143 distribution of the species in the Iberian Peninsula. The elevation of the sampled sites  
144 ranges from 1750 to 2451 m a.s.l. and the mean slope of the terrain is  $35^{\circ} \pm 16^{\circ}$  (see Table  
145 S1 in the Supplementary Material). Mean diameter at breast height (dbh) measured at 1.3  
146 m of sampled trees is  $66 \pm 7$  cm, and their age is  $334 \pm 108$  years on average (Table S1).

147 The location of the Pyrenees, between the Atlantic Ocean on the west side and the  
148 Mediterranean Sea in the east, causes a fast climatic transition, while the Central Pyrenees  
149 shows a greater continental influence (Del Barrio et al., 1990). In the western areas, most  
150 of the annual precipitation falls during the cold winter season, whereas precipitation falls  
151 mainly during spring and autumn in the east (Del Barrio et al., 1990). Air temperature  
152 changes depend on elevation with  $-5.17$  °C km<sup>-1</sup> being the mean temperature lapse rate

153 across the Pyrenees (Navarro-Serrano et al. 2018). The annual 0 °C isotherm is located at  
 154 2900 m a.s.l. (Del Barrio et al., 1990), whereas it falls to 1600 m a.s.l. between December  
 155 and April, establishing the lower limit of the seasonal snowpack (López-Moreno et al.,  
 156 2011). Snow accumulation also shows a correlation to Atlantic–Mediterranean proximity  
 157 and distance from the main divide of the mountain range (Revuelto et al., 2012). Monthly  
 158 mean values of temperature, snow depth and melt-out date from 1980 to 2009  
 159 hydrological years for all sampled sites are presented in Figure 1.

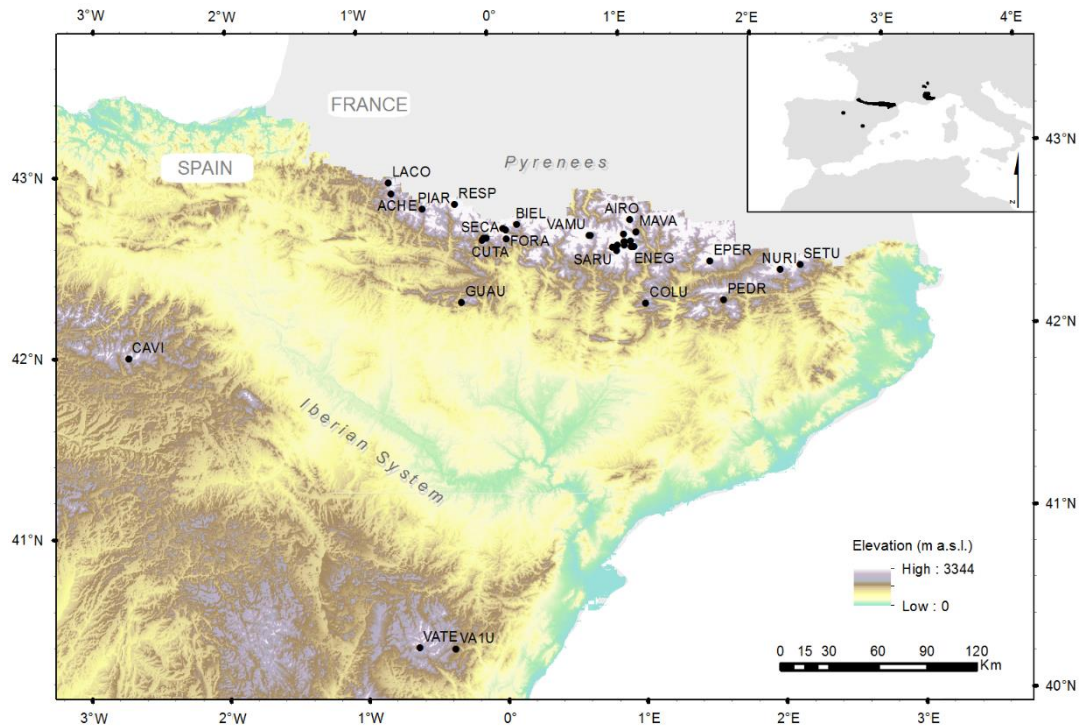
160



161

162 **Figure 1.** Top panel: Timing of *P. uncinata* tree-ring formation based on Camarero et al.  
 163 (1998). Red boxes indicate the most influencing months to *P. uncinata* radial growth by  
 164 temperature (Tardif et al., 2003; Galván et al., 2014). Bottom panels: monthly median  
 165 snow depth (SD, blue line), melt-out date frequency (MOD, bars) and monthly median  
 166 temperature (T, red line) of sampled sites in NE Iberian Peninsula from 1980 to 2009  
 167 hydrological years. Shaded areas show the 25-75 percentile ranks.

168



169

170 **Figure 2.** Map of sampled mountain *P. uncinata* sites in NE Iberian Peninsula (black  
 171 dots, see sites' codes in Table S1) and distribution of the study species in Europe (inset,  
 172 top right).  
 173

174 *2.3. Dendrochronological data*

175 Dendrochronological data correspond to an updating of data from 36 forests sampled and  
 176 published by Galván et al. (2012, 2014). Wood samples were collected between 1994 and  
 177 2010 from 5 to 65 dominant individual trees of different sizes and ages, randomly selected  
 178 in each site. From each tree, two or three cores were taken at 1.3 m height with Pressler  
 179 increment borers. The sapwood length was measured in the field, and topographic  
 180 (elevation, slope and aspect) and biometric (dbh and tree height) variables were also  
 181 recorded for each individual tree.

182 Wood samples were air dried and sanded until tree-ring boundaries were clearly  
 183 visible. Then, they were visually cross-dated and measured at 0.01 mm resolution using  
 184 a LINTAB measuring device (Rinntech, Heidelberg, Germany). Cross-dating quality was  
 185 checked using the program COFECHA (Holmes, 1983) by comparing the individual ring-



186 width series among coexisting trees of the same species. Finally, cross-dated tree-ring  
187 width (RWL) series were obtained.

188 Dimensionless ring-width indices (RWI) series were obtained by removing age or  
189 size trends and temporal autocorrelation to reflect growth response to climate. Residual  
190 RWIs were obtained by removing long-term trends of ring-width data fitting negative  
191 linear functions, followed by 30-year cubic smoothing splines, and then by eliminating  
192 the first-order autocorrelation of the resulting residuals using the software ARSTAN V.  
193 44 (Cook, 1985). A bi-weight robust mean was then computed to obtain residual or pre-  
194 whitened chronologies (mean site series) for each site, which were used in subsequent  
195 analyses.

#### 196 *2.4. Climatic and snow data*

197 Daily snow depth (SD) and temperature data (T) for the studied sites were extracted from  
198 a gridded meteorological dataset obtained by simulation from Weather Research and  
199 Forecasting (WRF; Skamarock et al., 2008) model. The WRF model was driven by ERA-  
200 Interim (Berrisford et al., 2011) reanalysis and coupled offline with Factorial Snow Model  
201 (FSM 1.0; Essery, 2015), a physically based energy and mass balance snow model. WRF  
202 outputs were projected to the target elevation, using hygrobarometric formulas and lapse  
203 rates and the new projected meteorological information as driving data of FSM. The  
204 methodology to develop the snow dataset and its validation is shown in Alonso-González  
205 et al. (2018).

206 Several annual snow indices were created from the daily snow data as indicators of  
207 specific snow conditions all year round, based on Figure 1:

- 208 - Average November snow depth (Nov SD) as previous autumn snow conditions  
209 indicator.
- 210 - Average February snow depth (Feb SD) as winter snow conditions indicator.

211 - Average May snow depth (May SD) as spring snow conditions indicator.

212 The selection of these monthly SD values for representing snow seasonal conditions  
213 is based on the cumulative nature of snow. Thus, the snow depth value at the end of the  
214 season will be representative of the accumulated snow and the meteorological conditions  
215 of the previous months (e.g. López-Moreno et al., 2005; Morán-Tejeda et al., 2016). Snow  
216 indices were not highly correlated with each other, showing an average coefficient of  
217 correlation lower than  $r_s = 0.55$  (Spearman Rho). Variables were detrended prior to the  
218 correlation analyses. Correlation coefficients ( $r_s$ ) were: 0.48 for Nov SD – Feb SD, 0.33  
219 for Nov SD – May SD and 0.54 for Feb SD – May SD.

220 Given that snow depth conditions of a given month are highly influenced by the  
221 temperature of previous months, the following monthly aggregations (averages) of  
222 temperature data were computed for statistical analyses: November mean temperature  
223 (Nov T), February mean temperature (Feb T), November-December-January-February  
224 mean temperature (Nov-Feb T), December-January-February mean temperature (Dec-  
225 Feb T), January-February mean temperature (Jan-Feb T), May mean temperature (May  
226 T), March-April-May mean temperature (Mar-May T), April-May mean temperature  
227 (Apr-May T).

228

## 229 2.5. Statistical analyses

230 We searched for snowpack effects on subsequent tree-ring development,  
231 considering the period from November (previous to tree-ring formation) to May, based  
232 on snow cover presence at the sampled forests (Figure 1).

233 The growing-season air temperature is a major and widely reported determinant of  
234 *P. uncinata* growth (Gutiérrez, 1991; Rolland and Schueller, 1994; Camarero et al., 1998;  
235 Tardif et al., 2003; Andreu et al., 2007; Galván et al., 2014). However, temperature also

236 determines the large variability of snowpack among elevations (López-Moreno, 2005;  
237 Morán-Tejeda et al., 2013b). Because the aim was to control the temperature effect on  
238 growth (RWI) and infer the pure effect of snow, the computed snow indices from the  
239 influence of temperature were isolated. This was done by considering the aforementioned  
240 snow depth and temperature indices as predictors of RWI by means of stepwise linear  
241 regressions. First, Spearman non-parametric correlations ( $r_s$ ) were computed between the  
242 snow depth indices (Nov SD, Feb SD, May SD) and the whole set of temperature monthly  
243 aggregations. Temperature aggregations that best correlated with snow indices were  
244 November T, Jan-Feb T and Mar-May T for Nov SD, Feb SD and May SD (See  
245 Supplementary Material Table S2). These best-correlated temperature aggregations,  
246 together with mean May temperature, because its influence on tree growth is widely  
247 reported as the most important (e.g., Tardif et al. 2003) and the snow depth indices were  
248 then used as predictors in the stepwise linear models (Eq. 1). The stepwise model allows  
249 introduction of variables that substantially improve the model by rejecting those that may  
250 be redundant. This prevents greatly auto-correlated variables from being included in the  
251 model and allowed us to infer whether the snow depth indices or temperature indices were  
252 the best predictors of RWI. Linear models were performed individually for each site, as  
253 well as a regional model for the whole set of sites. The models can be formulated as  
254 follows:

$$255 \quad y = \beta_0 + \beta_1 x_1 + \beta_2 x_2 + \dots + \beta_n x_n + \varepsilon \quad (\text{Eq. 1})$$

256 where  $y$  is the response variable (i.e. RWI values),  $\beta_0$  is the intercept,  $x_1$  to  $x_n$  are  
257 the predictors (i.e., snow depth and temperature indices),  $\beta_1$  to  $\beta_n$  are the estimated partial  
258 regression coefficients and  $\varepsilon$  is the error. The models were compared using the Akaike  
259 Information Criterion (AIC) value; the smaller the AIC, the better the fit (most  
260 parsimonious model) since it penalizes complex models (Burnham and Anderson, 2003).

261 Only the best model for each site and the one run for the whole set of sites are shown in  
262 the results, including the following information: the explained variance (adjusted  $R^2$ ), the  
263 statistical significance ( $p$ ) and the partial coefficients of the regressions. Automated  
264 model selection was performed with the MuMIn package (Barton and Barton, 2018) of  
265 the R language version 3.1.0 (R Core Team, 2014).

266 Additionally, partial correlations using the Spearman coefficient were calculated  
267 between RWI and SD indices by partially removing the effects of temperature (Table S2).  
268 Non-parametric methods were used, since not all analyzed variables had normal  
269 distributions (Shapiro–Wilk test,  $p < 0.05$ ). Snow and temperature variables were  
270 previously detrended.

271 Variations of tree growth responses to snow conditions along biogeographical  
272 gradients for a subset of sites where a snow index was the best predictor in the  
273 aforementioned stepwise models were investigated. The following variables were  
274 considered: latitude, longitude, slope, elevation of the terrain, dbh, tree height, sapwood  
275 and tree age (Table S1), and annual maximum snow depth (Max SD) (as an indicator of  
276 site differences in snow accumulation). Statistically significant different responses among  
277 groups of sites whose models selected the same best predictor using the non-parametric  
278 Kruskal-Wallis test were identified along gradients. Non-parametric Spearman  
279 correlations were calculated, considering the amount of radial growth variance explained  
280 by snow variables (adjusted  $R^2$  from the stepwise models) as the dependent variable and  
281 biogeographical gradients as independent variables. Complementary correlation analyses  
282 were done using partial correlation coefficients between tree growth and snow depth as  
283 dependent variables (in Supplementary Material Figure S3).

284 Trend analysis for tree-ring width (RWL series) as well as for snow indices was  
285 performed using the Mann-Kendall test and Theil-Sen's slope estimator for computing

286 the magnitude of the trend, considering a subset of sites where any snow – growth  
287 significant relationship was previously found. Trend analysis was carried out using the  
288 zyp package in R language (Bronaugh et al., 2009), which includes a trend-free pre-  
289 whitening method for removing serial autocorrelation.

290 RWI and RWL series were shorter than the snow series at some sites. Thus, all  
291 analyses were performed for the longest common period available, for example, from  
292 1981 to last formed tree-ring measured (number of available years for each one is  
293 indicated in Table S1).

294

### 295 **3. Results**

#### 296 *3.1. Growth responses to snow variables*

297 Stepwise linear models (Table 1) pointed out snow indices as main predictors of *P.*  
298 *uncinata* radial growth in 47% of sites (17 out of 36 sites; with 11 out of the 17 showing  
299 a statistically significant model). These 17 sites (Figure 3) were selected and used in later  
300 analyses. Average explained variance by models in these sites was 24% (30% for  
301 statistically significant models). The site in which predictors explained the larger variance  
302 of RWI was CONU (adjusted  $R^2 = 0.81$ ; Table 1). May SD was the best predictor in 64%  
303 of sites where snow indices were the most important predictors and their models were  
304 statistically significant (Figure 4). It was followed by Feb SD (selected in 27% of these  
305 sites) and Nov SD (only selected in one of these 11 sites). All snow indices negatively  
306 influenced radial growth (RWI) in all sites, except for Nov SD, which positively  
307 influenced tree radial growth in VA1U site.

308 In total, 17% of statistically significant models (6 out of 36 sites) pointed out  
309 temperature indices as main predictors of *P. uncinata* radial growth. Jan-Feb T was

310 selected as the best predictor of RWI in 5 out of 6 of these sites, and Mar-May T was  
 311 selected in only one site.

312 For the regional model, which takes into account all of the 36 site-chronologies  
 313 combined (Table 1, bottom), Nov SD was selected as the most important predictor  
 314 (despite it only explained 5% of the total variance). When a subset of statistically  
 315 significant sites was included in the general model, May SD was the most important  
 316 predictor again explaining 13% of the total growth variance.

317 Complementary to stepwise linear models, partial correlations also noted the  
 318 prevalence of Feb SD, with respect to the other two snow indices, in terms of influencing  
 319 radial growth of *P. uncinata* (Table S3 and Figure S1, Supplementary Material). Most  
 320 sites (67%) showed a Feb SD negative influence on radial growth (mean  $r_s = -0.34$ ; SD =  
 321 0.18), being five of them statistically significant. For May SD, one site showed  
 322 statistically significant partial correlation with radial growth.

323

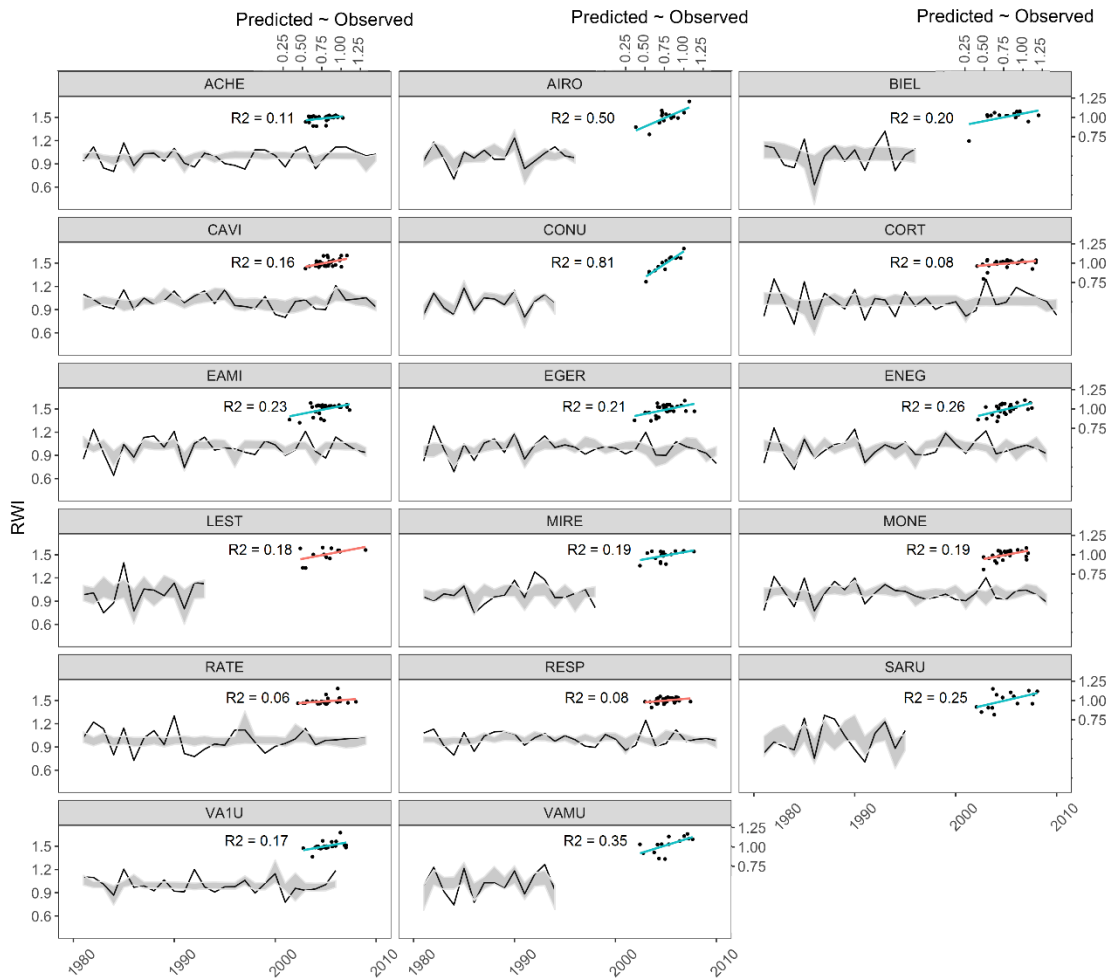
324 **Table 1.** Statistical parameters of stepwise linear models between radial growth (response  
 325 variable RWI) and snow and temperature indices (predictors) in each site, for all sites  
 326 (All sites), and for all statistically significant sites (Sig sites). See sites codes in Table S1  
 327 and Figure 2.

328

Site	N	Coefficients							Adjusted R <sup>2</sup>	P	
		Intercept	Nov SD	Feb SD	May SD	Nov T	May T	Jan-Feb T			Mar-May T
ACHE*	30	0.99			<b>-0.15</b>				0.11	0.041	
AIRO*	16	1.00			<b>-0.16</b>		0.04		0.50	0.019	
BIEL*	16	1.01			<b>-4.30</b>				0.20	0.046	
BLLA	30	0.99					0.03	<b>0.03</b>	0.25	0.098	
CAVI	30	1.01	<b>-0.36</b>	-0.07		0.02			0.16	0.090	
COLU	30								-		
CONU*	14	0.99	<b>-0.77</b>	-0.11	-0.56				-0.08	0.81	0.001
CORT	30	1.00			<b>-1.80</b>				0.08	0.072	
CUTA	17	1.00				<b>-0.03</b>			0.17	0.058	
EAMI*	29	1.00			<b>-0.55</b>				0.23	0.005	
EGER*	30	0.99			<b>-0.17</b>		0.02		0.21	0.019	
ELLA	29								-		
ENEG*	29	0.99			<b>-0.32</b>	-0.02			0.26	0.006	
EPER*	17	0.99					<b>0.07</b>		0.44	0.002	
FORA	29								-		
GUAU	30								-		
LACO	19								-		
LEST	13	1.00		<b>-0.29</b>					0.18	0.084	

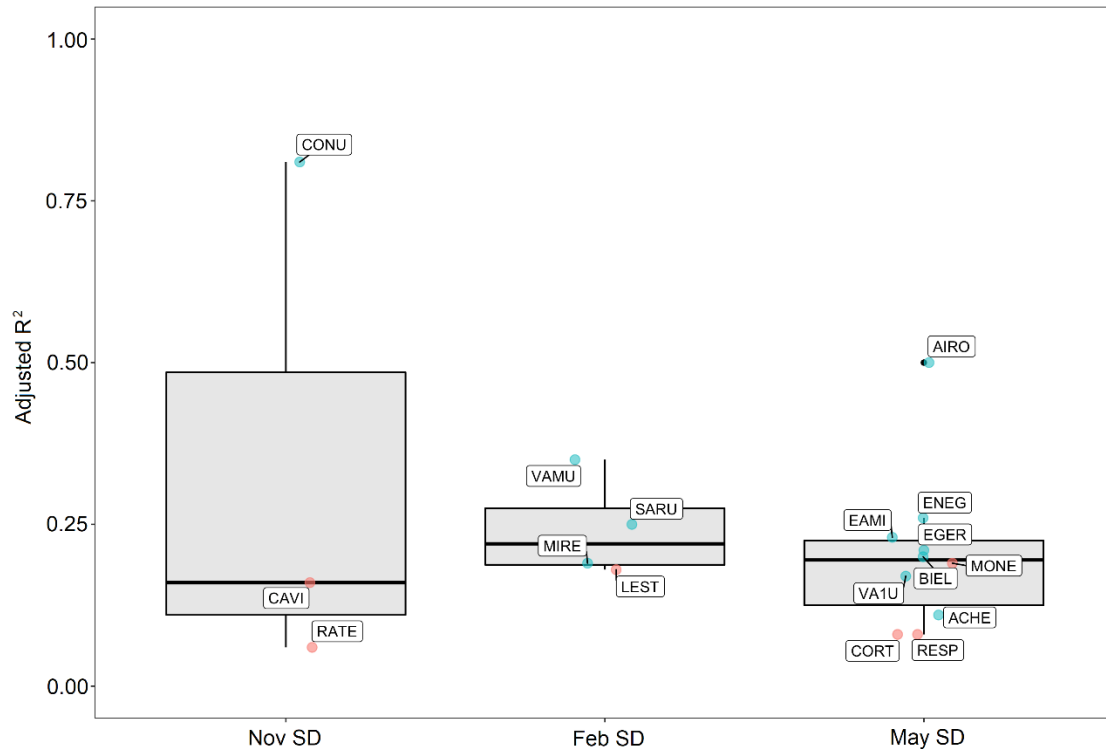
MAVA*	17	1.00					<b>0.09</b>		0.29	0.016	
MIRA	29	1.00						<b>0.05</b>	0.10	0.055	
MIRE*	18	0.99		<b>-0.18</b>					0.19	0.041	
MONE	29	1.00		<b>-0.08</b>	<b>-1.36</b>				0.19	0.082	
NURI*	21	0.99				-0.03		<b>0.05</b>	0.42	0.005	
PEDR	26	1.00						<b>0.03</b>	0.10	0.063	
PIAR	14	1.01						<b>0.04</b>	0.21	0.059	
RATE	29	0.99	<b>0.76</b>						0.06	0.109	
RESP	30	1.00						<b>-0.04</b>	0.08	0.071	
SAMA*	16	0.98						<b>0.08</b>	0.20	0.047	
SARU*	15	1.00		<b>-0.27</b>					0.25	0.034	
SECA	29								-		
SETU	19								-		
SOBR	29								-		
TESO*	15	0.97						<b>0.08</b>	0.28	0.024	
VA1U*	26	1.00	1.77						0.17	0.030	
VAMU*	14	1.02		<b>-0.23</b>					0.35	0.015	
VATE*	26	0.99							<b>0.08</b>	0.15	0.028
All sites	-	0.99	<b>0.08</b>	-0.03	-0.01	0.01	0.01	-0.01	0.05	0.00	
Sig sites	-	0.99		<b>-0.13</b>	-0.01	0.02	0.01	-0.01	0.13	0.00	

329 N: data series length starting from 1981 (years). Statistically significant sites (model  $p <$   
330 0.05) are followed by \*. The best predictor for each model (site) is indicated in bold  
331 characters. Hyphen indicates null models (any significant predictor).  
332  
333



334

335 **Figure 3.** Tree-ring width indices (RWI, lines) and confidence intervals (shaded areas)  
 336 stepwise linear models for selected sites. Scatter plots show correlatios between observed  
 337 and RWI values (right y-axes) predicted by the model (adjusted  $R^2$ ), and its statistical  
 338 significance (red: not significant; blue: significant,  $p < 0.05$ ).  
 339



340  
 341 **Figure 4.** Tree-growth variance (adjusted  $R^2$ ) explained by stepwise linear models for  
 342 selected sites. Values are displayed aggregated by best model predictor (snow indices  
 343 only). Sites related to each model are labelled. Statistical significance of models is  
 344 represented in red ( $p > 0.05$ ) and blue ( $p < 0.05$ ) colors. See sites codes in Table S1 and  
 345 Figure 2.  
 346

347 *3.2. Influence of biogeographical patterns and tree characteristics on growth responses*  
 348 *to snow depth.*

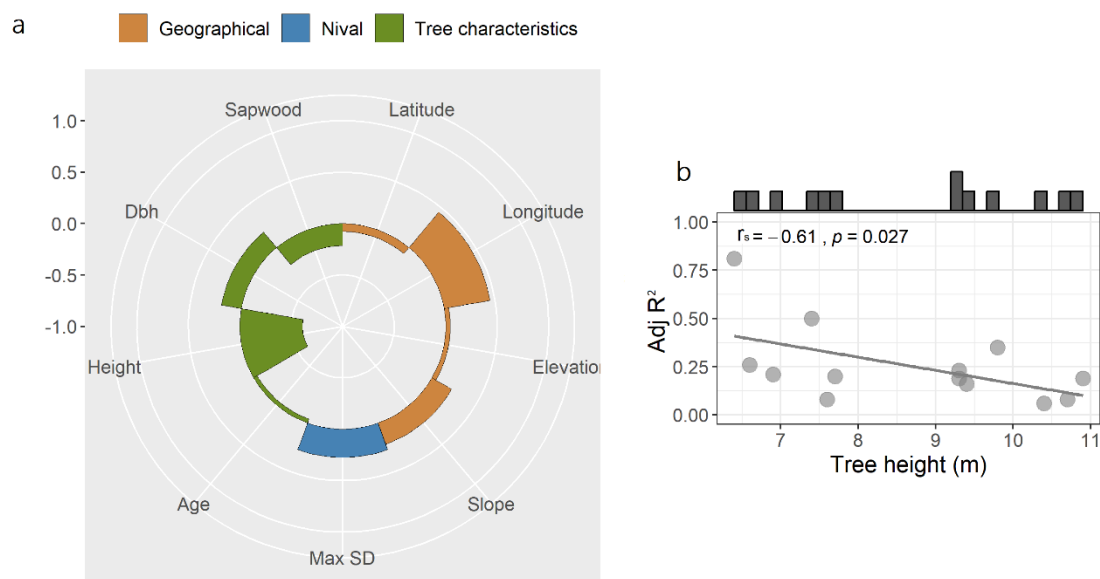
349 Tree characteristics determined the response of growth to snow (Fig 5a). The presence of  
 350 small trees strengthen the linkage between snow and growth in sites where a snow index  
 351 was the main driver of RWI ( $r_s = -0.61$ ,  $p = 0.03$ ) (Figure 5b). It was observed that sites  
 352 where a snow index was the statistically significant main driver of *P. uncinata* radial  
 353 growth were mostly located in the Pyrenees (at western and central area of this mountain  
 354 range), with the exception of one forest stand located in the southern Iberian System



355 (VA1U) (Fig S2). May SD was the main RWI predictor across the Pyrenees and also in  
356 the southern Iberian System site.

357 Additional biogeographical analyses based on growth-snow partial correlations  
358 showed that greater and statistically significant negative snow influence on tree growth  
359 was found in high-elevation sites (Nov SD index) and sites with bigger tree dbh (Feb SD  
360 index) (Figure S3).

361



362

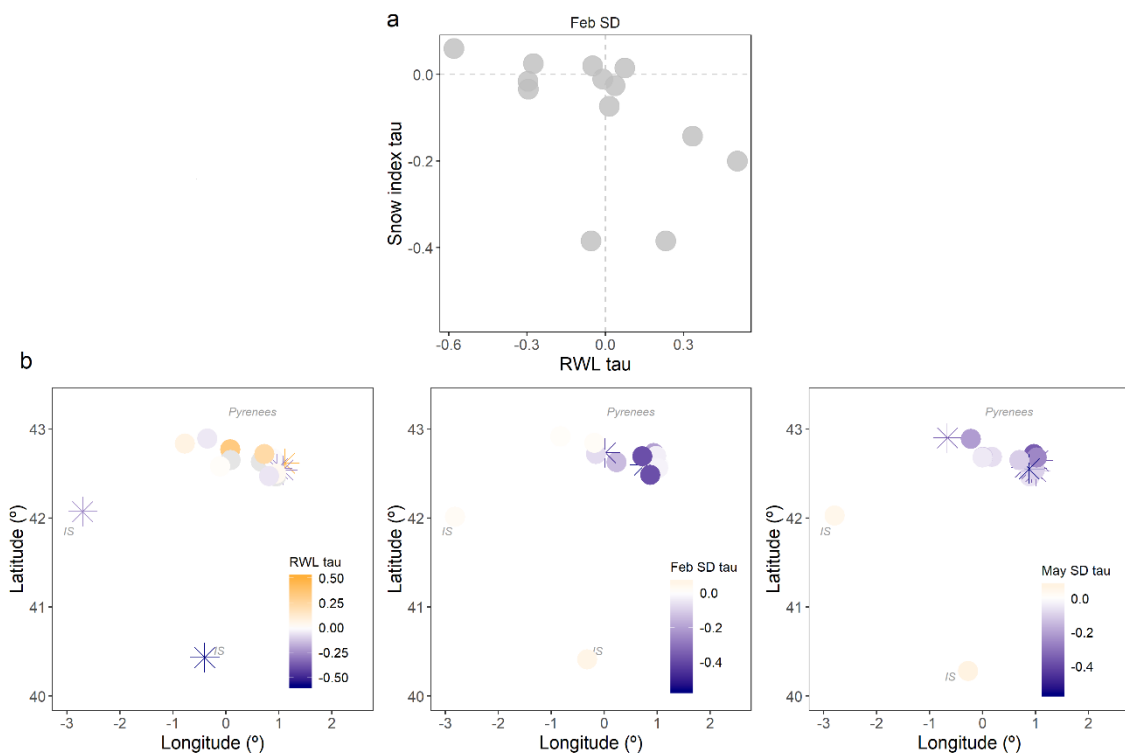
363 **Figure 5.** (a) Effects of geographical, nival gradients and tree influences on growth-snow  
364 variance (adjusted  $R^2$ ) established by Spearman correlations ( $r_s$ ). The southern Iberian  
365 System sites were omitted in latitude analyses. (b) Scatterplot of single obtained  
366 statistically significant correlation between growth-snow variance and biogeographical  
367 gradients (tree height) ( $p < 0.05$ ). Histograms show sites frequency of distribution along  
368 this gradient.

369

### 370 3.3. Tree radial growth and snow indices trend analysis

371 Five of thirteen forests presented statistically significant RWL trends, only one of them  
372 showed a positive slope for RWL trend while all the others showed a negative slope  
373 (Figure 6b; Figure S4). There were found statistically significant trends for May SD and  
374 Feb SD variables, in 35% and 12% of sites where snow index was the main driver of  $P$ .

375 *uncinata* radial growth respectively, but nor for Nov SD. All these statistically significant  
 376 snow trends show negative slopes.  
 377 A statistically significant correlation was found between growth trends (RWL) and snow  
 378 (Feb SD) trends ( $r_s = -0.68$ ;  $p = 0.01$ ) (Figure 6a). From the regional perspective, only in  
 379 the Pyrenees there were found statistically significant trends in snow variables (all of  
 380 them with negative coefficients as mentioned above).



381 **Figure 6.** (a) Mann-Kendall linear trends (tau) for tree-ring width (RWL) and Feb SD  
 382 snow index of selected sites from 1981 to last year with data (see series' lengths in Table  
 383 S1) and (b) geographical representation of trend analyses results. Pyrenees and Iberian  
 384 System (IS) locations are indicated.  
 385  
 386

#### 387 4. Discussion

388 There is evidence that previous snow cover conditions influence *P. uncinata* tree-ring  
 389 formation, in addition to the widely reported growing season air temperature effects, as  
 390 hypothesized. The used methodology allowed us to infer the pure effect of snow on tree-  
 391 ring growth by controlling the temperature influence on snowpack evolution. First, the  
 392 most correlated monthly temperature aggregations to snow indices were detected (Table

393 S2), including other key temperature indices (May T) for *P. uncinata* growth; second,  
394 both temperature and snow indices were taken into account as predictors in radial growth  
395 stepwise linear models and by using partial correlations as complementary analyses.  
396 Similar procedures were used in Carlson et al. (2017) and Helama et al. (2013). Results  
397 provide additional information about the effects of climate on high-elevation *P. uncinata*  
398 radial growth. Previous studies showed that radial growth of *P. uncinata* was mainly  
399 limited by growing-season air temperature (Rolland and Schueller, 1994; Camarero et al.,  
400 1998; Tardif et al., 2003; Andreu et al., 2007; Galván et al., 2014) and, only in certain  
401 drought-prone sites, by low early summer precipitation (Andreu et al., 2007; Galván et  
402 al., 2014).

403 The influence of snow cover on radial growth had not been researched for *P.*  
404 *uncinata*, but it has been researched for other species of Pinaceae (Walsh et al., 1994;  
405 Kirdyanov et al., 2003; Helama et al., 2013; Watson and Luckman, 2016; Carlson et al.,  
406 2017; Franke et al., 2017; Appleton and St. George, 2018; Fkiri et al., 2018; Legendre-  
407 Fixx et al., 2018; Truettner et al., 2018). In this study, almost half the sampled forests in  
408 the main mountain ranges of the NE Iberian Peninsula showed certain snow-growth  
409 interaction (most of them were statistically significant).

410 The date of cambial initiation is a key factor for climate-growth associations. This  
411 date is related to the date when snowmelt occurs (Kirdyanov et al., 2003) and,  
412 consequently, with snow accumulation throughout the winter. The presence of abundant  
413 snowpack in late spring may induce a late melt-out and, as a result, a delay in the onset  
414 of the *P. uncinata* growing season because the persistent snow cover may cool the soil  
415 (Kirdyanov et al., 2003; Helama et al., 2013). This would explain the dominant negative  
416 spring snow (May SD index) influence on *P. uncinata* annual growth found in this study  
417 (Table 1, Figure 4). In this regard, Franke et al. (2017) reported that the average monthly

418 snow cover during the current year's May correlated negatively with *P. sylvestris*  
419 chronologies. Likewise, northern conifers showed delayed cambial activity when snow  
420 melt was delayed in the beginning of the growing season (Vaganov et al., 1999;  
421 Kirilyanov et al., 2003). Previous studies of *P. uncinata* have demonstrated that this pine  
422 species is negatively affected by the preceding growing-season low air temperatures  
423 because the onset of cambial activity is triggered by a typical rise in temperature during  
424 spring (Tardif et al., 2003; Galvan et al., 2014). Since no positive relation was found  
425 between May SD snow index and RWI series in the performed models, we cannot report  
426 that moisture from spring snowmelt promotes annual growth of *P. uncinata* in sampled  
427 forests. The positive influence of snow on tree growth, explained by a moisture-  
428 limitation, widely reported in more arid places as well as in large snow accumulation  
429 areas (St. George, 2014; Watson and Luckman, 2016; Carlson et al., 2017), was not  
430 detected in the few possible drought-prone sites (Pre-Pyrenees and southern Iberian  
431 System) sampled in this study. Winter precipitation is less likely to contribute to the soil  
432 moisture reservoir used by trees during the following growing season if spring  
433 precipitation is abundant and shows low year-to-year variability as is the case. Spring  
434 rainfalls would introduce an extra source of water that would sum up to the water from  
435 snowmelt, and thus, the positive influence of snow on tree growth based on moisture-  
436 limitation was not detected.

437 As discussed above, large winter snow accumulation likely produces larger snow  
438 presence in spring and this, in turn, causes a delayed melt-out. It is not easy to isolate the  
439 impact of winter snow on radial growth, compared to that of late spring snow, because  
440 they both are related; however, we did observe that May SD was selected 60% more than  
441 Feb SD as best predictor of RWI in the performed models (Table 1). In this regard,  
442 Watson and Luckman (2016) evidenced a relation between larger snow accumulation and

443 delays in *P. ponderosa* and *Pseudotsuga menziesii* growing seasons in some regions of  
444 Canada. Fkiri et al. (2018) also reported that winter snow is a major factor limiting growth  
445 of *P. nigra* in NW Tunisia. Other studies, however, pointed to a positive influence of  
446 winter snowfall on tree-ring growth due to snowmelt waters may constitute much of the  
447 available resource to trees during the beginning of the following growing season (e.g. St.  
448 George, 2014).

449 A possible explanation for the scarce influence of preceding November snow  
450 conditions on growth observed in our study is that occasional early-season snowfalls  
451 before November did not contribute to overall autumn snow accumulation, thus it was  
452 relegated to accumulation occurred in the season last month. As a consequence, small  
453 snowpacks were found in November. Furthermore, this late autumn snow depth  
454 accumulation has a minor influence on the presence of late spring snow (Nov SD and  
455 May SD indices were not correlated,  $r_s = 0.33$ ), which was pointed out in this study as  
456 the most important seasonal snow component influencing *P. uncinata* growth. Contrary  
457 to our results, Carlson et al. (2017) in *P. albicaulis* forests and Helama et al. (2013) in *P.*  
458 *sylvestris* forests detected significant negative effects of autumn snowfall and autumn  
459 snow depth on radial growth, respectively. The early snowfall in autumn and soil cooling  
460 can be related to the cessation and shortening of the growing season (Carlson et al., 2017).  
461 In this instance, other physiological tree processes are affected: among others, (1) the  
462 reduction of photosynthate storage for the following year growth resumption (Fritts,  
463 1976), (2) the reduction of mycorrhizal activity (Peterson and Peterson, 1994), and (3)  
464 the inhibition of carbon transfer into radial growth and later carbon storage for the  
465 following year (Hoch and Körner, 2003). Moreover, previous studies have demonstrated  
466 that *P. uncinata* is sensitive to previous November low temperatures, when synthesis and

467 storage of carbohydrates can affect later radial growth (Tardif et al., 2003; Galván et al.,  
468 2014).

469 Evidence of tree characteristics' influence on the snow-radial growth relationship  
470 was found. Smaller trees showed to be more sensitive to snow effects (Figure 5b), which  
471 could be due to a more efficient hydraulic functioning (Galván et al. 2012) or to a lower  
472 influence of snowpack on microclimate and phenology in the case of tall trees. Zhu et al.  
473 (2015) reported that large trees have higher recovery rates from snow damage than  
474 smaller trees. With regard to geographical distribution of snow-growth interactions, in  
475 the Pyrenean sites (central and western areas) occurred almost all of the significant snow-  
476 growth correlations, but also the negative snow-growth influence was detected in the drier  
477 Iberian System site. Any snow influence on *P. uncinata* growth was found in the Pre-  
478 Pyrenees or eastern Pyrenees sampled sites. Previous studies (Tardif et al., 2003; Galván  
479 et al., 2014) have demonstrated that elevation plays a major role in *P. uncinata* radial  
480 growth-index responses to climate. Galván et al. (2014) observed an elevation pattern  
481 regarding temperature: November temperature conditions during the year prior to tree-  
482 ring formation influence *P. uncinata* growth mainly in mid-elevation sites, whereas at  
483 higher elevations, growth was more dependent on May temperature conditions during the  
484 year of tree-ring formation. However, no statistical significant relation was found  
485 regarding the elevation gradient determine whether *P. uncinata* radial growth is  
486 influenced by a specific snow index. Thought results from partial correlation analyses  
487 indicate that the main negative snow influences on tree growth were found at higher  
488 elevations (Figure S3), this study did not produce sufficient evidence to confirm our initial  
489 hypothesis. We expected that upper and therefore colder forest sites could be the most  
490 sensitive to snow-growth influences. The decrease in near-surface air temperature  
491 produced by an increase in elevation (Navarro-Serrano et al., 2018) was suggested to limit

492 the maximum elevation of tree growth due to a short growing season (Körner, 2012).  
493 Consequently, snow conditions could be expected to be the most limiting factor for radial  
494 growth at high elevations which further reduces *P. uncinata* growth period, especially  
495 linked to late spring snow cover. But more detailed information on elevational gradients  
496 of snow features are needed to test it.

497 Significant and decreasing trends were detected in winter and spring snow depths  
498 along the Pyrenees (although trend coefficients are very dependent on the selected study  
499 period), similar to other main mid-latitude mountain ranges (López-Moreno, 2005;  
500 Marty, 2008; McCabe and Wolock, 2009; Beniston, 2012; Morán-Tejeda et al., 2013a;  
501 Buisan et al., 2015) (Figure 6b). A significant and negative response of *P. uncinata*  
502 growth to the negative trends in winter snow was found (Figure 6a), but it was not  
503 ubiquitous. Thus, trends of *P. uncinata* growth were not consistent through all forests,  
504 though almost all the statistically significant coefficients found were negative (only there  
505 was one increasing growth trend). This may be related, however, to the length of the radial  
506 growth data series. Overall results suggest that *P. uncinata* radial growth could benefit  
507 from the predicted shallower snowpack in these mountain ranges (López-Moreno, 2005;  
508 Morán-Tejeda et al., 2013a) over the next decades by a prolongation of the growing  
509 season, especially in high elevation forests. Likewise, climatic warming is expected to  
510 promote forest growth in the Pyrenees in a similar way (Tardif et al., 2003). However,  
511 growth could be declined in some dry sites where the amount of soil water available to  
512 trees in the growing season relates to the previous months' snowpack (Pederson et al.,  
513 2011). Therefore, in xeric sites, a shallower snowpack due to warmer temperatures could  
514 lead to limited soil water content in spring and reduce growth (Walsh et al., 1994;  
515 Truettner et al., 2018). It has been reported that these thermal stress sites are dependent  
516 on early summer precipitation (Richter et al., 1991; Andreu et al., 2007; Galván et al.,

517 2014), but this has not been observed so far in our studied sites. This may be related to  
518 limitation in the data used in this study. The length of the radial growth data series was  
519 not consistent throughout the sampled sites, ranging from 30 to 13 years of available data  
520 per sampled forest. The temperature and snow depth data were a product of a climate  
521 simulation with the WRF model, with a spatial resolution (10 x 10 km) that could be too  
522 coarse to represent their real spatial variability on the complex terrains of the forests. The  
523 regional nature of this study prevented consideration with finer-scale climatic  
524 observations.

525 This study seeks to further research with higher spatial and temporal resolution  
526 data, including in-situ climatic and snow cover records, and other environmental variables  
527 (such as soil moisture, wind, and solar radiation) in order to improve understanding of  
528 how snow-growth relations occur in *P. uncinata* mountain forests.

529

## 530 **5. Conclusions**

531 Radial growth of *P. uncinata* forests is affected by snow cover depth, independent of the  
532 widely reported effect of growing season air temperature on their wood formation. *P.*  
533 *uncinata* growth is negatively influenced by a larger winter and late spring snowpack  
534 depth. Geographical and topographical gradients and some tree characteristics as height  
535 explained differences in snow–growth relationships. This study suggests that a future  
536 shallower and more transitory snowpack in the studied mountains may benefit the growth  
537 of *P. uncinata* over the next decades, although a few forests could experience warming-  
538 induced drought stress.



539 **Funding**

540 This study was funded by the Spanish Ministry of Economy and Competitiveness [grant  
541 numbers CGL2014-52599-P, CGL2017-82216-R]. A. Sanmiguel-Vallelado is supported  
542 by a University Professor Training grant [grant number FPU16/00902] funded by the  
543 Spanish Ministry of Education, Culture and Sport.

544

545 **Acknowledgements**

546 We thank all management personnel and forest guards connected to the National Parks  
547 or protected areas sampled in this study for their support. We also thank AEMET and  
548 CHE for providing climate data.

549

550 **References**

- 551 Alonso-González, E., López-Moreno, J.I., Gascoin, S., García-Valdecasas Ojeda, M.,  
552 Sanmiguel-Valladolid, A., Navarro-Serrano, F., Revuelto, J., Ceballos, A.,  
553 Esteban-Parra, M.J., Essery, R., 2018. Daily gridded datasets of snow depth and  
554 snow water equivalent for the Iberian Peninsula from 1980 to 2014. *Earth Syst.*  
555 *Sci. Data* 10, 303–315. <https://doi.org/10.5194/essd-10-303-2018>
- 556 Andreu, L., Gutiérrez, E., Macias, M., Ribas, M., Bosch, O., Camarero, J.J., 2007.  
557 Climate increases regional tree-growth variability in Iberian pine forests. *Glob.*  
558 *Change Biol.* 13, 804–815. <https://doi.org/10.1111/j.1365-2486.2007.01322.x>
- 559 Appleton, S.N., St. George, S., 2018. High-elevation mountain hemlock growth as a  
560 surrogate for cool-season precipitation in Crater Lake National Park, USA.  
561 *Dendrochronologia* 52, 20–28. <https://doi.org/10.1016/j.dendro.2018.09.003>
- 562 Barton, K., Barton, M.K., 2018. Package ‘MuMIn.’ Model selection and model  
563 averaging based on information criteria. R package version 3.5.1. R Foundation  
564 for Statistical Computing, Vienna, Austria.
- 565 Beniston, M., 2003. Climatic change in mountain regions: a review of possible impacts,  
566 in: *Climate Variability and Change in High Elevation Regions: Past, Present &*  
567 *Future*. Springer, 5–31.
- 568 Beniston, M., 2012. Is snow in the Alps receding or disappearing? *Wiley Interdiscip.*  
569 *Rev. Clim. Change* 3, 349–358. <https://doi.org/10.1002/wcc.179>
- 570 Beniston, M., Uhlmann, B., Goyette, S., Lopez-Moreno, J.I., 2011. Will snow-abundant  
571 winters still exist in the Swiss Alps in an enhanced greenhouse climate? *Int. J.*  
572 *Climatol.* 31, 1257–1263. <https://doi.org/10.1002/joc.2151>
- 573 Berrisford, P., Dee, P., Poli, R., Brugge, K., Fielding, M., Fuentes, P., Kallberg, S.,  
574 Kobayashi, S., Uppala, Simmons, A., 2011. The ERA-Interim archive version

575 2.0. ERA Rep. Ser., 23.

576 Bronaugh, D., Werner, A., Bronaugh, M.D., 2009. Package ‘zyp.’ CRAN Repos.

577 Buisán, S. T., Saz Sánchez M.A., López-Moreno, J.I, 2015. Spatial and temporal  
578 variability of winter snow and precipitation days in the western and central  
579 Spanish Pyrenees. *Int. J. Climatol.* 35, 259-274.  
580 <https://doi.org/10.1002/joc.3978>.

581 Burnham, K.P., Anderson, D.R., 2003. Model selection and multimodel inference: a  
582 practical information-theoretic approach. Springer Science & Business Media.

583 Camarero, J. J., Gazol, A., Galván, J.D., Sanguesa-Barreda, G., Gutiérrez., E., 2015a.  
584 Disparate effects of global-change drivers on mountain conifer forests:  
585 warming-induced growth enhancement in young trees vs. CO<sub>2</sub> fertilization in  
586 old trees from wet sites. *Glob. Change Biol.* 21: 738–749.  
587 <https://doi.org/10.1111/gcb.12787>.

588 Camarero, J.J., Gazol, A., Sancho-Benages, S. and Sanguesa-Barreda, G., 2015b. Know  
589 your limits? Climate extremes impact the range of Scots pine in unexpected  
590 places. *Ann. Bot.* 116: 917–927. <https://doi.org/10.1093/aob/mcv124>

591 Camarero, J.J., Gazol, A., Tardif, J.C. and Conciatori, F. 2015c. Attributing forest  
592 responses to global-change drivers: limited evidence of a CO<sub>2</sub>-fertilization  
593 effect in Iberian pine growth. *J. Biogeogr.* 42: 2220–2233.

594 Camarero, J.J., Guerrero-Campo, J., Gutiérrez, E., 1998. Tree-ring growth and structure  
595 of *Pinus uncinata* and *Pinus sylvestris* in the Central Spanish Pyrenees. *Arct.*  
596 *Alp. Res.* 30, 1–10.

597 Camarero, J.J., Linares, J.C., García-Cervigón, A.I., Batllori, E., Martínez, I., Gutiérrez,  
598 E., 2017. Back to the future: the responses of alpine treelines to climate warming  
599 are constrained by the current ecotone structure. *Ecosystems* 20, 683–700.

600 <https://doi.org/10.1007/s10021-016-0046-3>

601 Cantegrel, R., 1983. Le Pin à crochets pyrénéen: biologie, biochimie, sylviculture. *Acta*  
602 *Biol. Mont.* 2, 87–330.

603 Carlson, K.M., Coulthard, B., Starzomski, B.M., 2017. Autumn snowfall controls the  
604 annual radial growth of centenarian whitebark pine (*Pinus albicaulis*) in the  
605 southern Coast Mountains, British Columbia, Canada. *Arct. Antarct. Alp. Res.*  
606 49, 101–113. <https://doi.org/10.1657/AAAR0016-033>

607 Cook, E.R., 1985. A time series analysis approach to tree ring standardization  
608 (dendrochronology, forestry, dendroclimatology, autoregressive process).  
609 Dissertation, The University of Arizona.

610 D’Orangeville, L., Houle, D., Duchesne, L., Phillips, R. P., Bergeron, Y., Kneeshaw,  
611 D., 2018. Beneficial effects of climate warming on boreal tree growth may be  
612 transitory. *Nat. Commun.*, 9(1), 3213. DOI: 10.1038/s41467-018-05705-4

613 Del Barrio, G., Creus, J., Puigdefábregas, J., 1990. Thermal seasonality of the high  
614 mountain belts of the Pyrenees. *Mt. Res. Dev.* 227–233.

615 El Kenawy, A., López-Moreno, J.I., Vicente-Serrano, S.M., 2011. Recent trends in daily  
616 temperature extremes over northeastern Spain (1960–2006). *Nat. Hazards Earth*  
617 *Syst. Sci.* 11, 2583–2603. <https://doi.org/10.5194/nhess-11-2583-2011>

618 Essery, R., 2015. A factorial snowpack model (FSM 1.0). *Geosci. Model Dev.* 8(12),  
619 3867–3876. doi:10.5194/gmd-8-3867-2015

620 Fkiri, S., Guibal, F., Fady, B., Khorchani, A.E., Khaldi, A., Khouja, M.L., Nasr, Z.,  
621 2018. Tree-rings to climate relationships in nineteen provenances of four black  
622 pines sub-species (*Pinus nigra* Arn.) growing in a common garden from  
623 Northwest Tunisia. *Dendrochronologia* 50, 44–51.  
624 <https://doi.org/10.1016/j.dendro.2018.05.001>

625 Franke, A.K., Bräuning, A., Timonen, M., Rautio, P., 2017. Growth response of Scots  
626 pines in polar-alpine tree-line to a warming climate. *For. Ecol. Manag.* 399, 94–  
627 107. <https://doi.org/10.1016/j.foreco.2017.05.027>

628 Fritts, H.C., 1976. *Tree rings and Climate*. Acad. San Diego Calif., 567 pp.

629 Galván, D.J., Büntgen, U., Ginzler, C., Grudd, H., Gutiérrez, E., Labuhn, I. and  
630 Camarero, J.J. 2015. Drought-induced weakening of growth-temperature  
631 associations in high-elevation Iberian pines. *Glob. Planet. Ch.* 124, 95–106.

632 Galván, J.D., Camarero, J.J., Gutiérrez, E., 2014. Seeing the trees for the forest: drivers  
633 of individual growth responses to climate in *Pinus uncinata* mountain forests. *J.*  
634 *Ecol.* 102, 1244–1257. <https://doi.org/10.1111/1365-2745.12268>

635 Galván, J.D., Camarero, J.J., Sangüesa-Barreda, G., Alla, A.Q., Gutiérrez, E., 2012.  
636 Sapwood area drives growth in mountain conifer forests. *J. Ecol.* 100, 1233–  
637 1244. <https://doi.org/10.1111/j.1365-2745.2012.01983.x>

638 García-Ruiz, J.M., Puigdefábregas, T.J., Creus-Novau, J., 1985. Los recursos hídricos  
639 superficiales del Alto Aragón. Instituto de Estudios Altoaragoneses, 224 pp.

640 Gutiérrez, E., 1991. Climate-tree-growth relationships for *Pinus uncinata* Ram. in the  
641 Spanish pre-Pyrenees. *Acta Oecol.* 12, 213–225.

642 Helama, S., Mielikainen, K., Timonen, M., Herva, H., Tuomenvirta, H., Venalainen, A.,  
643 2013. Regional climatic signals in Scots pine growth with insights into snow and  
644 soil associations. *Dendrobiology* 70: 27–34.  
645 <http://dx.doi.org/10.12657/denbio.070.003>

646 Hoch, G., Körner, C., 2003. The carbon charging of pines at the climatic treeline: a  
647 global comparison. *Oecologia* 135, 10–21. [https://doi.org/10.1007/s00442-002-](https://doi.org/10.1007/s00442-002-1154-7)  
648 [1154-7](https://doi.org/10.1007/s00442-002-1154-7)

649 Holmes, R.L., 1983. Computer-assisted quality control in tree-ring dating and

650 measurement. *Tree-Ring Bull.*

651 Innes, J.L., 1991. High-altitude and high-latitude tree growth in relation to past, present  
652 and future global climate change. *The Holocene* 1: 168–173.  
653 <https://doi.org/10.1177/095968369100100210>.

654 Kirilyanov, A., Hughes, M., Vaganov, E., Schweingruber, F., Silkin, P., 2003. The  
655 importance of early summer temperature and date of snow melt for tree growth  
656 in the Siberian Subarctic. *Trees* 17, 61–69. [https://doi.org/10.1007/s00468-002-](https://doi.org/10.1007/s00468-002-0209-z)  
657 [0209-z](https://doi.org/10.1007/s00468-002-0209-z)

658 Körner, C., 2012. *Alpine Treelines: Functional Ecology of the Global High Elevation*  
659 *Tree Limits*. Springer.

660 Legendre-Fixx, M., Anderegg, L.D.L., Ettinger, A.K., HilleRisLambers, J., 2018. Site-  
661 and species-specific influences on sub-alpine conifer growth in Mt. Rainier  
662 National Park, USA. *Forests* 9, 1. <https://doi.org/10.3390/f9010001>

663 López-Moreno, J.I., 2005. Recent variations of snowpack depth in the Central Spanish  
664 Pyrenees. *Arct. Antarct. Alp. Res.* 37, 253–260. [https://doi.org/10.1657/1523-](https://doi.org/10.1657/1523-0430(2005)037[0253:RVOSDI]2.0.CO;2)  
665 [0430\(2005\)037\[0253:RVOSDI\]2.0.CO;2](https://doi.org/10.1657/1523-0430(2005)037[0253:RVOSDI]2.0.CO;2)

666 López-Moreno, J.I., Morán-Tejeda, E., Vicente Serrano, S.M., Lorenzo-Lacruz, J.,  
667 García-Ruiz, J.M., 2011. Impact of climate evolution and land use changes on  
668 water yield in the Ebro basin. *Hydrol. Earth. Syst. Sci.* 15, 311–322.  
669 <http://dx.doi.org/10.5194/hess-15-311-2011>

670 López-Moreno, J.I., Vicente-Serrano, S.M., Angulo-Martínez, M., Beguería, S.,  
671 Kenawy, A., 2010. Trends in daily precipitation on the northeastern Iberian  
672 Peninsula, 1955–2006. *Int. J. Climatol.* 30, 1026–1041.  
673 <https://doi.org/10.1002/joc.1945>

674 Marty, C., 2008. Regime shift of snow days in Switzerland. *Geophys. Res. Lett.* 35,

675 L12501. <https://doi.org/10.1029/2008GL033998>

676 McCabe, G.J., Wolock, D.M., 2009. Recent declines in western US snowpack in the  
677 context of twentieth-century climate variability. *Earth Interact.* 13, 1–15.  
678 <https://doi.org/10.1175/2009EI283.1>

679 Morán-Tejeda, E., Herrera, S., López-Moreno, J.I., Revuelto, J., Lehmann, A.,  
680 Beniston, M., 2013a. Evolution and frequency (1970–2007) of combined  
681 temperature–precipitation modes in the Spanish mountains and sensitivity of  
682 snow cover. *Reg. Environ. Change* 13, 873–885. [https://doi.org/10.1007/s10113-](https://doi.org/10.1007/s10113-012-0380-8)  
683 [012-0380-8](https://doi.org/10.1007/s10113-012-0380-8)

684 Morán-Tejeda, E., López-Moreno, J. I., Stoffel, M., Beniston, M., 2016. Rain-on-snow  
685 events in Switzerland: recent observations and projections for the 21st century.  
686 *Clim. Res.* 71, 111–125. <https://doi.org/10.3354/cr01435>

687 Morán-Tejeda, E., López-Moreno, J.I., Beniston, M., 2013b. The changing roles of  
688 temperature and precipitation on snowpack variability in Switzerland as a  
689 function of altitude. *Geophys. Res. Lett.* 40, 2131–2136.  
690 <https://doi.org/10.1002/grl.50463>

691 Morán-Tejeda, E., López-Moreno, J.I., Sanmiguel-Valladolid, A., 2017. Changes in  
692 climate, snow and water resources in the Spanish Pyrenees: observations and  
693 projections in a warming climate, in: Catalan, J., Ninot, J. M., Aniz, M. M.  
694 (Eds.), *High Mountain Conservation in a Changing World*. Springer, pp. 305–  
695 323.

696 Morán-Tejeda, E., Lorenzo-Lacruz, J., López-Moreno, J.I., Rahman, K., Beniston, M.,  
697 2014. Streamflow timing of mountain rivers in Spain: recent changes and future  
698 projections. *J. Hydrol.* 517, 1114–1127.  
699 <https://doi.org/10.1016/j.jhydrol.2014.06.053>

700 Navarro-Serrano, F., I. López-Moreno, J., Azorin-Molina, C., Alonso-González, E.,  
701 Tomás-Burguera, M., Sanmiguel-Valladolid, A., Revuelto, J., Beguería, S., 2018.  
702 Estimation of near-surface air temperature lapse rates over continental Spain and  
703 its mountain areas. *Int. J. Climatol.* 38, 3233–3249.  
704 <https://doi.org/10.1002/joc.5497>

705 Pederson, G.T., Gray, S.T., Woodhouse, C.A., Betancourt, J.L., Fagre, D.B., Littell,  
706 J.S., Watson, E., Luckman, B.H., Graumlich, L.J., 2011. The Unusual Nature of  
707 Recent Snowpack Declines in the North American Cordillera. *Science* 333, 332–  
708 335. <https://doi.org/10.1126/science.1201570>

709 Peterson, D.W., Peterson, D.L., 1994. Effects of climate on radial growth of subalpine  
710 conifers in the North Cascade Mountains. *Can. J. For. Res.* 24, 1921–1932.  
711 <https://doi.org/10.1139/x94-247>

712 R Core Team, 2014. R: A language and environment for statistical computing. R  
713 Foundation for Statistical Computing, Vienna, Austria.

714 Revuelto, J., López-Moreno, J.I., Morán Tejada, E., Fassnacht, S., Serrano, V., Martín,  
715 S., 2012. Variabilidad interanual del manto de nieve en el Pirineo: tendencias  
716 observadas y su relación con índices de teleconexión durante el periodo 1985-  
717 2011, in: Rodríguez, C., Ceballos, A., González, N., Morán-Tejada, E., Pacheco  
718 S., Hernández, A. (Eds.), *Cambio climático. Extremos e impactos*. Asociación  
719 Española de Climatología, Salamanca, pp. 613–621.

720 Rolland, C., Schueller, J.F., 1994. Relationships between mountain pine and climate in  
721 the French Pyrenees (Font-Romeu) studied using the radiodensitometrical  
722 method. *Pirineos* 143, 55–70. [https://doi.org/10.3989/pirineos.1994.v143-](https://doi.org/10.3989/pirineos.1994.v143-144.156)  
723 [144.156](https://doi.org/10.3989/pirineos.1994.v143-144.156)

724 Sanchez-Salguero, R., Camarero, J., Gutiérrez, E., Gazol, A., Sangüesa-Barreda, G.,



725 Moiseev, P., Linares, J., 2018. Climate Warming Alters Age-Dependent Growth  
726 Sensitivity to Temperature in Eurasian Alpine Treelines. *Forests* 9, 688. DOI:  
727 10.3390/f9110688

728 Sánchez-Salguero, R., Navarro-Cerrillo, R.M., Swetnam, T.W., Zavala, M.A., 2012. Is  
729 drought the main decline factor at the rear edge of Europe? The case of southern  
730 Iberian pine plantations. *For. Ecol. Manage.* 271, 158–169.  
731 <https://doi.org/10.1016/j.foreco.2012.01.040>

732 Sangüesa-Barreda, G., Camarero, J.J., Esper, J., Galván, J.D., Büntgen, U., 2018. A  
733 millennium-long perspective on high-elevation pine recruitment in the Spanish  
734 central Pyrenees. *Can. J. For. Res.* 1113, 1108–1113.

735 Skamarock, W. C., Klemp, J. B., Dudhia, J., Gill, D. O., Barker, D. M., Dudha, M. G.,  
736 Huang, X., Wang, W., Powers, Y., 2008. A Description of the Advanced  
737 Research WRF Version 3. NCAR Tech. Note NCAR/TN-475+STR.  
738 <https://doi.org/10.5065/D68S4MVH>

739 Smithers, B.V., North, M.P., Millar, C.I., Latimer, A.M., 2018. Leap frog in slow  
740 motion: Divergent responses of tree species and life stages to climatic warming  
741 in Great Basin subalpine forests. *Glob. Change Biol.* 24, 442–457.  
742 <https://doi.org/10.1111/gcb.13881>

743 St. George, S., 2014. An Overview of Tree-Ring Width Records across the Northern  
744 Hemisphere. *Quat. Sci. Rev.* 95, 132–150.  
745 <https://doi.org/10.1016/j.quascirev.2014.04.029>.

746 Tardif, J., Camarero, J.J., Ribas, M., Gutiérrez, E., 2003. Spatiotemporal variability in  
747 tree growth in the Central Pyrenees: climatic and site influences. *Ecol. Monogr.*  
748 73, 241–257. [https://doi.org/10.1890/0012-](https://doi.org/10.1890/0012-9615(2003)073[0241:SVITGI]2.0.CO;2)  
749 [9615\(2003\)073\[0241:SVITGI\]2.0.CO;2](https://doi.org/10.1890/0012-9615(2003)073[0241:SVITGI]2.0.CO;2)

750 Truettner, C., Anderegg, W.R.L., Biondi, F., Koch, G.W., Ogle, K., Schwalm, C.,  
751 Litvak, M.E., Shaw, J.D., Ziaco, E., 2018. Conifer radial growth response to  
752 recent seasonal warming and drought from the southwestern USA. *For. Ecol.*  
753 *Manage.* 418, 55–62. <https://doi.org/10.1016/j.foreco.2018.01.044>

754 Vaganov EA, Hughes MK, Kirilyanov AV, Schweingruber FH, Silkin PP. 1999.  
755 Influence of snowfall and melt timing on tree growth in subarctic Eurasia.  
756 *Nature* 400: 149–151. <https://doi.org/10.1038/22087>

757 Walsh, S.J., Butler, D.R., Allen, T.R., Malanson, G.P., 1994. Influence of snow patterns  
758 and snow avalanches on the alpine treeline ecotone. *J. Veg. Sci.* 5, 657–672.  
759 <https://doi.org/10.2307/3235881>

760 Wang, X., Pederson, N., Chen, Z., Lawton, K., Zhu, C., Han, S., 2019. Recent rising  
761 temperatures drive younger and southern Korean pine growth decline. *Sci. Total*  
762 *Environ.* 649, 1105–1116. DOI: 10.1016/j.scitotenv.2018.08.393

763 Watson, E., Luckman, B.H., 2016. An investigation of the snowpack signal in moisture-  
764 sensitive trees from the Southern Canadian Cordillera. *Dendrochronologia* 38,  
765 118–130. <https://doi.org/10.1016/j.dendro.2016.03.008>

766 Zhu, L., Zhou, T., Chen, B., Peng, S., 2015. How does tree age influence damage and  
767 recovery in forests impacted by freezing rain and snow? *Sci. China Life Sci.* 58,  
768 472–479. <https://doi.org/10.1007/s11427-014-4722-2>

769 Zhuang, L., Axmacher, J.C., Sang, W., 2017. Different radial growth responses to  
770 climate warming by two dominant tree species at their upper altitudinal limit on  
771 Changbai Mountain. *J. For. Res.* 28, 795–804. [https://doi.org/10.1007/s11676-](https://doi.org/10.1007/s11676-016-0364-5)  
772 [016-0364-5](https://doi.org/10.1007/s11676-016-0364-5)

773

775 **Table S1.** *Pinus uncinata* sampled sites and their geographical, topographical, ecological  
776 and nival characteristics. Values are means  $\pm$  standard deviation.  
777

Mountain range	Site (code)	Analysed years	Latitude N (°)	Longitude -W, +E (°)	Elevation (m a.s.l.)	Slope (°)	dbh (cm)	Age (years)	Max SD (m)
	Acherito (ACHE)	30	42.89	-0.75	1850	–	–	–	2.31 $\pm$ 0.61
	Airoto (AIRO)	16	42.70	1.03	2300	47 $\pm$ 29	58.5 $\pm$ 13.5	288 $\pm$ 100	2.54 $\pm$ 0.70
	Bielsa (BIEL)	16	42.70	0.18	2000	88 $\pm$ 4	45.1 $\pm$ 9.4	270 $\pm$ 67	1.14 $\pm$ 0.36
	Barranc de Llacs (BLLA)	30	42.53	0.92	2250	44 $\pm$ 38	71.7 $\pm$ 20.0	616 $\pm$ 175	2.65 $\pm$ 0.86
	Conangles (CONU)	14	42.62	0.73	2106	43 $\pm$ 15	56 $\pm$ 14.5	318 $\pm$ 117	1.94 $\pm$ 0.61
	Corticelles-Dellu� (CORT)	30	42.56	0.93	2269	24 $\pm$ 17	83.1 $\pm$ 28.8	509 $\pm$ 177	1.26 $\pm$ 0.47
	Las Cutas (CUTA)	17	42.62	-0.08	2150	20 $\pm$ 5	33.3 $\pm$ 8.3	129 $\pm$ 16	1.31 $\pm$ 0.49
	Estany d’Amitges (EAMI)	29	42.58	0.98	2390	40 $\pm$ 21	69 $\pm$ 26.0	355 $\pm$ 106	1.51 $\pm$ 0.59
	Estany Gerber (EGER)	30	42.62	0.98	2268	15 $\pm$ 15	53.5 $\pm$ 14.6	426 $\pm$ 147	2.24 $\pm$ 0.64
	Estany de Lladres (ELLA)	29	42.55	1.05	2120	35 $\pm$ 12	52.1 $\pm$ 9.8	313 $\pm$ 123	1.03 $\pm$ 0.54
	Estany Negre (ENEG)	29	42.55	1.03	2451	35 $\pm$ 18	71 $\pm$ 26.0	411 $\pm$ 182	1.68 $\pm$ 0.66
	Estansys de la Pera (EPER)	17	42.45	1.61	2360	30 $\pm$ 0	65.2 $\pm$ 11.0	339 $\pm$ 117	0.94 $\pm$ 0.39
	Foratarruego (FORA)	29	42.62	0.10	2031	37 $\pm$ 11	49.5 $\pm$ 18.3	433 $\pm$ 50	1.83 $\pm$ 0.83
	Larra (LACO)	19	42.95	-0.77	1750	38 $\pm$ 24	46.4 $\pm$ 14.0	350 $\pm$ 108	1.90 $\pm$ 0.53
Pyrenees	La Estiva (LEST)	13	42.68	0.08	2000	–	–	–	1.10 $\pm$ 0.32
	Mata de Val�ncia (MAVA)	17	42.63	1.07	2019	19 $\pm$ 10	43.2 $\pm$ 3.6	237 $\pm$ 72	1.65 $\pm$ 0.58
	Mirador (MIRA)	29	42.58	0.98	2180	33 $\pm$ 18	55.1 $\pm$ 25.8	401 $\pm$ 132	1.06 $\pm$ 0.41
	Mirador del Rey (MIRE)	18	42.63	-0.07	1980	25 $\pm$ 10	53.3 $\pm$ 15.3	117 $\pm$ 18	0.94 $\pm$ 0.29
	Monestero (MONE)	29	42.56	0.98	2280	28 $\pm$ 13	64.4 $\pm$ 16.1	346 $\pm$ 110	1.28 $\pm$ 0.49
	Vall de N�ria (NURI)	21	42.38	2.13	2075	–	–	–	0.49 $\pm$ 0.27
	Pic d’Arnousse (PIAR)	14	42.80	-0.52	1940	32 $\pm$ 4	65.4 $\pm$ 5.1	248 $\pm$ 83	2.80 $\pm$ 0.67
	Ratera (RATE)	29	42.58	0.98	2170	40 $\pm$ 5	28.3 $\pm$ 8.1	380 $\pm$ 146	1.04 $\pm$ 0.40
	Respomuso (RESP)	30	42.82	-0.28	2350	70 $\pm$ 19	49.5 $\pm$ 15.1	280 $\pm$ 83	4.61 $\pm$ 1.17
	Sant Maurici (SAMA)	16	42.58	0.98	1933	16 $\pm$ 15	38.2 $\pm$ 5.7	204 $\pm$ 23	0.67 $\pm$ 0.22
	Sarrad� (SARU)	15	42.55	0.89	1950	–	–	–	1.65 $\pm$ 0.51
	Senda de Cazadores (SECA)	29	42.63	-0.05	2247	49 $\pm$ 12	60.9 $\pm$ 16.5	337 $\pm$ 145	1.60 $\pm$ 0.76
	Setcases (SETU)	19	42.40	2.28	2080	–	–	–	0.68 $\pm$ 0.35
	Sobrestivo (SOBR)	29	42.67	0.10	2296	38 $\pm$ 2	61.7 $\pm$ 17.5	341 $\pm$ 97	2.06 $\pm$ 0.88
	Tess� de Son (TESO)	15	42.58	1.03	2239	42 $\pm$ 14	74.5 $\pm$ 18.8	346 $\pm$ 202	1.15 $\pm$ 0.37
	Vall de Mulleres (VAMU)	14	42.62	0.72	1800	34 $\pm$ 13	69 $\pm$ 26.0	437 $\pm$ 184	1.27 $\pm$ 0.35
	Cap de Boumort (COLU)	30	42.23	1.12	1915	–	–	–	0.35 $\pm$ 0.22
Pre-Pyrenees	Guara (GUAU)	30	42.28	-0.25	1790	–	–	–	0.62 $\pm$ 0.32
	Pedraforca (PEDR)	26	42.23	1.70	2100	–	–	–	0.69 $\pm$ 0.37
Iberian System	Vinuesa (CAVI)	30	42.00	-2.73	2050	21 $\pm$ 1	85.6 $\pm$ 23.0	368 $\pm$ 148	1.31 $\pm$ 0.39
	Valdelinares (VATE-VAIU)	26	40.37	-0.37	1955	10 $\pm$ 5	63.8 $\pm$ 12.4	214 $\pm$ 107	0.57 $\pm$ 0.32

779 **Table S2.** Coefficients from Spearman correlations ( $r_s$ ) between snow indices and  
 780 temperature monthly aggregations. Arrow indicates which monthly aggregation of  
 781 temperature is best correlated to each snow index and is then used in further analysis.

782

Temperature indices	Snow indices		
	Nov SD	Feb SD	May SD
Nov T	-0.34** ←		
Feb T		-0.63**	
Nov-Feb T		-0.57**	
Dec-Feb T		-0.63**	
Jan-Feb T		-0.64** ←	
May T			-0.55**
Mar-May T			-0.57** ←
Apr-May T			-0.56**

783 Values followed by \*\* are statistically significant at  $p < 0.01$ .

784

785

786  
787  
788

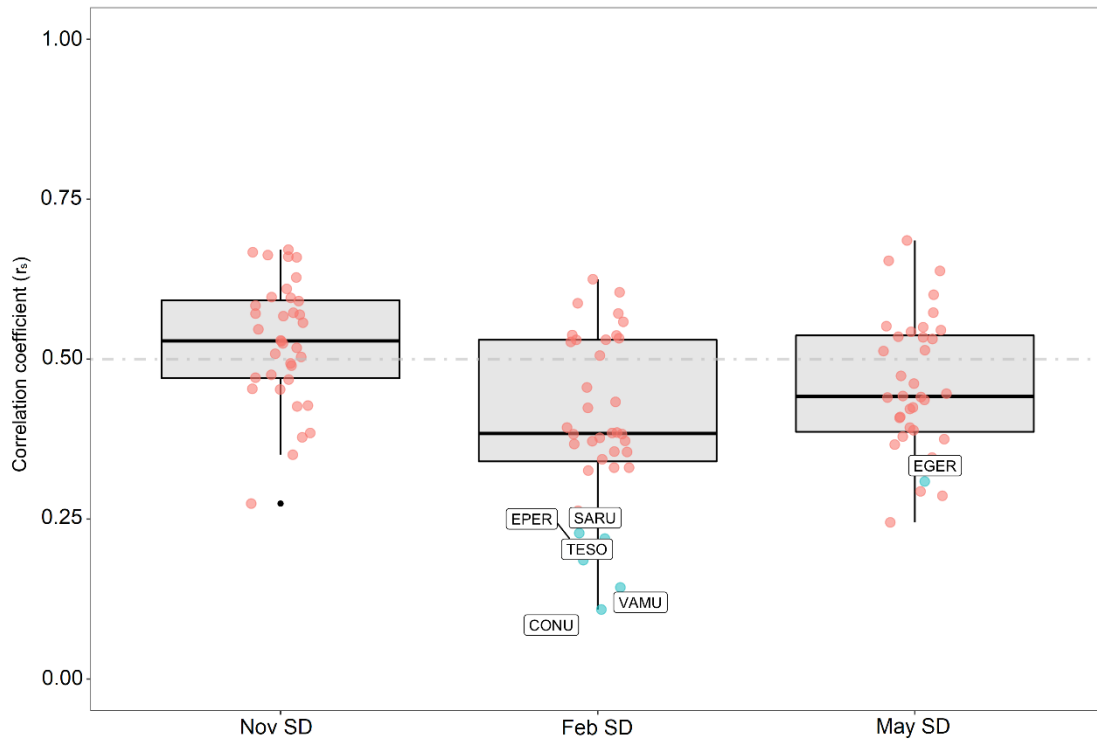
**Table S3.** Correlation coefficients from partial correlations calculated between tree-ring width and snow indices.

Site	N° analysed years	Spearman correlations coefficients ( $r_s$ )		
		Nov SD	Feb SD	May SD
ACHE	30	-0.09	-0.27	-0.22
AIRO	16	-0.24	-0.23	-0.41
BIEL	16	0.32	-0.34	-0.12
BLLA	30	0.09	-0.09	-0.13
CAVI	30	-0.23	-0.35	-0.33
COLU	30	0.01	0.14	0.03
CONU	14	-0.06	-0.78**	-0.51
CORT	30	-0.02	-0.26	-0.18
CUTA	17	-0.30	0.01	0.07
EAMI	29	0.14	-0.23	0.03
EGER	30	0.05	-0.29	-0.38*
ELLA	29	0.19	0.21	-0.16
ENEG	29	0.06	-0.23	-0.12
EPER	17	-0.45	-0.56*	0.09
FORA	29	0.15	0.06	0.20
GUAU	30	0.13	0.17	0.06
LACO	19	0.22	-0.25	-0.31
LEST	13	0.14	-0.31	0.31
MAVA	17	0.17	0.08	0.15
MIRA	29	0.06	-0.23	-0.05
MIRE	18	-0.05	-0.47	0.37
MONE	29	0.02	-0.26	-0.21
NURI	21	0.11	-0.13	0.09
PEDR	26	0.04	-0.21	-0.25
PIAR	14	0.32	0.07	0.28
RATE	29	0.33	0.12	-0.24
RESP	30	-0.15	-0.15	-0.27
SAMA	16	0.33	0.05	-0.43
SARU	15	-0.06	-0.54*	-0.12
SECA	29	0.26	0.25	0.10
SETU	19	-0.15	0.07	-0.11
SOBR	29	-0.09	-0.29	-0.08
TESO	15	-0.01	-0.63*	-0.18
VAIU	26	0.34	0.06	0.07
VAMU	14	0.19	-0.71**	0.10
VATE	26	0.18	-0.34	-0.15

789  
790  
791

Values followed by \* and \*\* are statistically significant at  $p < 0.05$  and  $p < 0.01$ , respectively. Note that data length differs between sites.

792 **Figure S1.** Partial correlation coefficients (Spearman,  $r_s$ ) calculated between tree-ring  
793 width and snow indices. Sites where a statistically significant correlation was found are  
794 labelled. Statistical significance of models is represented in red ( $p > 0.05$ ) and blue ( $p <$   
795  $0.05$ ) colors.

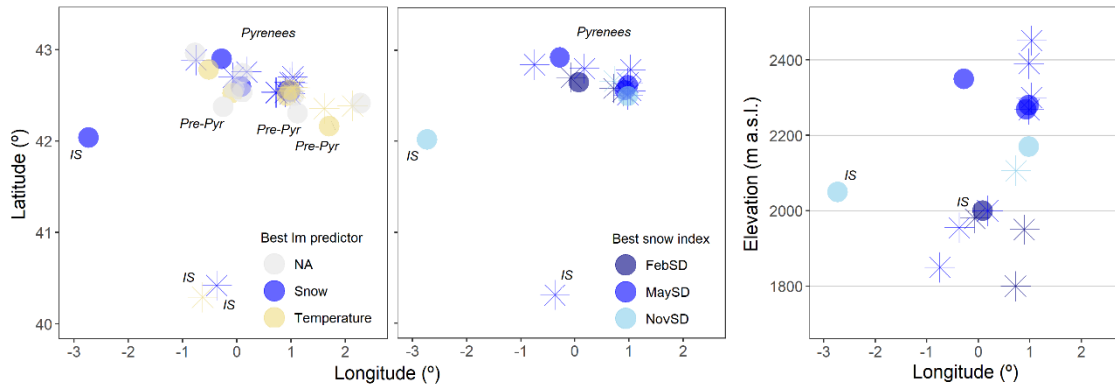


796

797

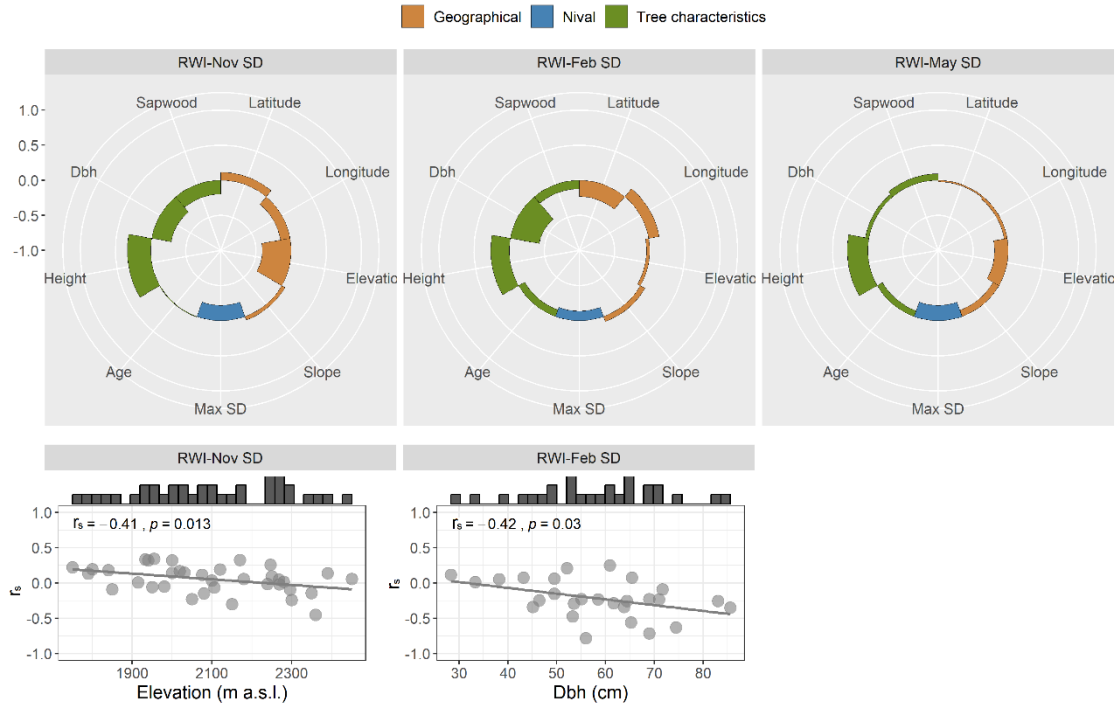
798

799 **Figure S2.** Latitude, longitude and elevation distribution patterns for groups of sites with  
 800 the same RWI main drivers. Pre-Pyrenees (Pre-Pyr) and Iberian System (IS) locations are  
 801 indicated where applicable. NA indicates sites whose selected model was null. Stars  
 802 indicate sites whose selected model was statistically significant ( $p < 0.05$ ).  
 803



804  
 805

806 **Figure S3.** (a) Effect of geographical, nival gradients and tree influences on growth-snow  
 807 partial correlations (Spearman correlations,  $r_s$ ). The southern Iberian System sites were  
 808 omitted in latitude analyses. (b) Scatterplots of statistically significant correlations ( $p <$   
 809  $0.05$ ) obtained between growth-snow partial correlations and biogeographical gradients.  
 810 Histograms show sites frequency of distribution along gradients.  
 811



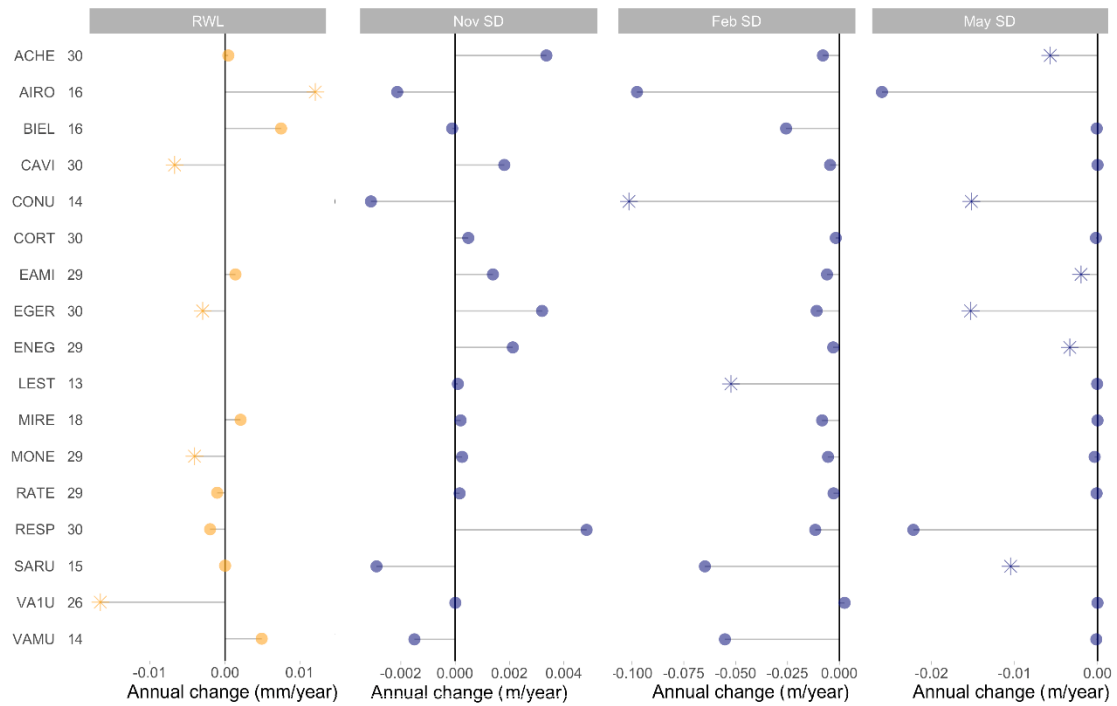
812

813

814



815 **Figure S4.** Theil-Sen's slopes (variable's units in  $\text{mm}\cdot\text{year}^{-1}$ ) for tree-ring width (RWL)  
 816 and snow indices trends of selected sites from 1981 to last year with data (series' lengths  
 817 are shown after site codes). Statistically significant values at  $p < 0.05$  are represented  
 818 with stars. Blank values in RWL mean data is not available for these sites.



819

820